Journal of Inclusion Phenomena and Molecular Recognition in Chemistry **11**: 215–224, 1991.

Thermodynamic Analysis of Equilibria between Binary Liquid and Solid Solutions in Ternary Systems. Application to Systems in which Two Guests Compete for Sites in the Same Host, Tetrakis(4-Methylpyridine)Nickel(II) Isothiocyanate

NORMAN O. SMITH
Department of Chemistry, Fordham University, Bronx, NY 10458-5198, U.S.A.

(Received: 17 December 1990)

Abstract. A thermodynamic analysis is presented of the equilibria between liquid solutions of guest A in guest B and solid solutions of HA in HB, where HA and HB are isomorphous 1:1 compounds of these guests with the host H. (The treatment is applicable whether or not HA and HB are inclusion compounds.) The mole ratio of A to B in the liquid, R_l, is generally different from the same ratio in the solid, R_s. Data on many systems have indicated a linear relation between $\ln R_l$ and $\ln R_s$, but to date no theoretical basis has been forthcoming. The present analysis shows that this relation is usually sigmoidal in shape but, with certain restrictions, is nearly linear. The slope and intercept are interpreted in terms of the equilibrium constant for the displacement of A from HA by B and the deviations from ideality in the liquid and solid phases.

If the deviations from ideality in the liquid phase are known or can be estimated, those for the solid phase can be determined, and thermodynamic equilibrium constants and standard free energy changes for the displacement of A by B calculated. These methods were applied to available data for the following pairs of guests with the host $Ni(4\text{-mepy})_4(NCS)_2$: *p*-xylene with each of *p*-dibromobenzene, *p*-xylene-d_6, *p*-xylene-d_{10}, *p*-bromotoluene, *p*-chlorotoluene, *p*-dichlorobenzene, *p*-fluorotoluene, ethylbenzene, toluene, and benzene, and the pairs *p*-dichlorobenzene/*p*-chlorotoluene and ethylbenzene/toluene.

Key words. Thermodynamics of guest competition, $Ni(4\text{-mepy})_4(NCS)_2$.

1. Introduction

The host tetrakis(4-methylpyridine)nickel(II) isothiocyanate (H) forms numerous isomorphous inclusion compounds with liquid aromatic guests [1, 2, 3, 4, 5]. When excess of two such guests, A and B, are equilibrated with H, two phases are formed: a solid solution of the compound of H with A, HA, in the compound of H with B, HB, and a liquid solution of A in B. The systems considered below are those in which H is usually insoluble in A and B and in which HA and HB are 1:1 inclusion compounds, but the treatment is applicable regardless of the crystal structure of HA and HB.

The phase behaviour is shown in Figure 1. It is seen that the guests are distributed between liquid and solid phases, but that the ratios of A to B in the two phases are different, causing the tie lines to be skewed. Some of the studies [2] have been strictly isothermal, many [3, 4, 5] have been at 'room temperature', and two [3] have been in the presence of a cosolvent. The resulting data are reported as R_l and

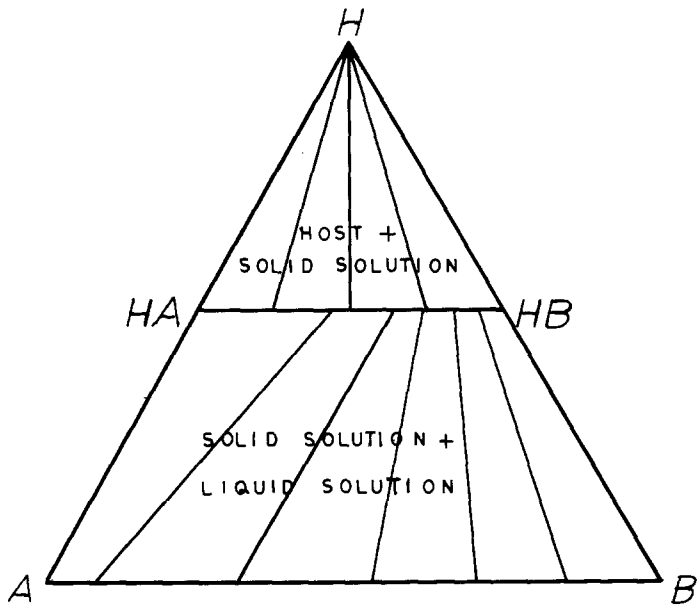

Fig. 1. Schematic isotherm for a system of two guests competing for the same host.

R_s, R_l is the mole ratio of A to B in the liquid phase and R_s is the ratio in the solid phase. When $\ln R_l$ as abscissa is plotted against $\ln R_s$ as ordinate the data always seem to fall on a straight line within experimental error, so that

$$\ln R_s = m \ln R_l + b \tag{1}$$

Considering the high probability that the coexisting solutions, especially the solid ones, are not ideal, this fact was always surprising, and the present study was undertaken to find the reason for the apparent linearity. Another objective was to determine whether the experimental data could be used to yield such thermodynamic data as equilibrium constants connected with the distribution phenomena. Lipkowski and co-workers [5] had indicated that the intercept on the $\ln R_s$ axis of the above-mentioned plot "may be used as a direct measure of the thermodynamic constant of clathration equilibria" – a concept which seemed to this author to be too simple to be true, except as a limiting case.

Although most of the data used were not obtained under strictly isothermal conditions it was assumed in what follows that they were for a temperature of about 25°C. It was felt that temperature fluctuations of $\pm 5°$ would be unimportant compared with experimental error, particularly as the guests were covalent substances.

2. Distribution Equilibria

The equilibria can be formulated as a distribution of each guest between liquid and solid phases: A (in liquid solution) $\rightleftharpoons$ A (in solid solution) and B (in liquid solution) $\rightleftharpoons$ B (in solid solution). Alternatively, since the solid phase is a binary

solid solution, one may formulate the equilibrium as HA (solid soln) + B (liquid soln) $\rightleftharpoons$ HB (solid soln) + A (liquid soln) where H is the host, HA and HB are the isomorphous 1:1 inclusion compounds of the (binary) solid phase, and A and B are the components of the (binary) liquid phase. The thermodynamic equilibrium constant, K, can then be expressed in terms of mole fractions, x, and activity coefficients, γ, as $K = (x_{HB(s)}\gamma_{HB(s)}x_{A(l)}\gamma_{A(l)})/(x_{HA(s)}\gamma_{HA(s)}x_{B(l)}\gamma_{B(l)})$. This will be rewritten for brevity, as

$$K = (R_l/R_s)(\gamma_{HB}/\gamma_{HA})(\gamma_A/\gamma_B) \tag{2}$$

where R_l is the ratio of the mole fractions of A to B in the liquid phase, R_s is the ratio of the mole fractions of HA to HB in the solid phase, γ_A and γ_B refer to the liquid phase and γ_{HA} and γ_{HB} to the solid. The standard states for A and B in the liquid will be the respective pure liquids; the standard states for HA and HB will be the respective pure solid HA and HB.

If, as a limiting case, both the solid and liquid phases are ideal, that is, if HA and HB follow Raoult's law in the solid and A and B follow it in the liquid phase, then the activity coefficients are all unity and Equation (2) reduces to $K = R_l/R_s$, or

$$\ln R_s = \ln R_l - \ln K \tag{3}$$

Thus $m = 1$ and $b = -\ln K$ in Equation (1), and b *is* a measure of K. Such a limiting case demands that the separation factor, $s = R_s/R_l$, be constant for all relative amounts of A and B, a situation which would appear to be unlikely unless A and B are very similar.

Equation (2), on taking logarithms, yields

$$\ln R_s = \ln R_l + \ln(\gamma_{HB}/\gamma_{HA}) - \ln(\gamma_B/\ln \gamma_A) - \ln K \tag{4}$$

When $x_{A(l)}$ and $x_{A(s)}$ approach unity and therefore R_l and R_s become very large, both γ_{HB}/γ_{HA} and γ_B/γ_A approach constant values, regardless of the functional form used to express the concentration dependence of the activity coefficients. Equation (4), therefore, approaches

$$\ln R_s = \ln R_l + \text{constant} \tag{5}$$

Similarly, when $x_{A(l)}$ and $x_{A(s)}$ approach zero the activity coefficient ratios approach (different) constant values, and Equation (4) approaches

$$\ln R_s = \ln R_l + \text{constant} \tag{6}$$

It follows that all plots of $\ln R_s$ against $\ln R_l$ eventually become straight lines with unit slope in both directions, but the two linear portions have, in general, different intercepts. The shape of the line which joins the two limiting straight portions will be discussed immediately below.

It will now be assumed that the activity coefficients in both phases can be expressed, at least approximately, by the '2-suffix Margules' equations [6]

$$\ln \gamma_A = B_l x_{B(l)}^2; \qquad \ln \gamma_B = B_l x_{A(l)}^2 \tag{7}$$

$$\ln \gamma_{HA} = B_s x_{HB}^2; \qquad \ln \gamma_{HB} = B_s x_{HA}^2 \tag{8}$$

where B_l and B_s are constants. These comply with the Gibbs–Duhem requirement

but imply a symmetry in the concentration dependence in both phases. Positive deviations from Raoult's law in the liquid phase give $B_l > 0, \gamma > 1$; negative deviations give $B_l < 0, \gamma < 1$. Analogous statements are true for the solid phase.

If the liquid solutions are ideal or nearly so, $B_l = 0$ and, from Equations (8), $\ln(\gamma_{HB}/\gamma_{HA}) = B_s(x_{HA}^2 - x_{HB}^2) = B_s(x_{HA} - x_{HB})$ since $x_{HA} + x_{HB} = 1$. Equation (2) then becomes

$$\ln s = B_s(x_{HA} - x_{HB}) - \ln K \tag{9}$$

A plot of $\ln s$ against $x_{HA} - x_{HB}$ then gives a straight line with slope B_s and intercept $-\ln K$.

If the liquid solutions are not ideal, but if γ_A and γ_B can be determined by some method, then, setting $s' = (R_s/R_l)(\gamma_B/\gamma_A)$ in Equation (2), yields

$$\ln K = \ln(\gamma_{HB}/\gamma_{HA}) - \ln s' \tag{10}$$

which, with the help of Equations (8), gives

$$\ln s' = B_s(x_{HA} - x_{HB}) - \ln K \tag{11}$$

This resembles Equation (9) to which it reduces when the liquid solutions are ideal. A plot of $x_{HA} - x_{HB}$ against $\ln s'$ should, in this event, be linear and yield B_s, the solid phase activity coefficients, and K. If the plot is smooth but not straight the approach described immediately below is suggested.

Alternatively, if the activity coefficients in the liquid are available, and if the distribution data are of sufficiently good quality, γ_{HA} and γ_{HB} can be expressed by the '3-suffix Margules' equations [7] as $\ln \gamma_{HA} = Bx_{HB}^2 + Cx_{HB}^3$ and $\ln \gamma_{HB} = (B + \frac{3}{2}C)x_{HA}^2 - Cx_{HA}^3$, where B and C are constants. Subtracting the first of these equations from the second and substituting into Equation (10) gives, on simplification, the polynomial

$$\ln s' = -\tfrac{3}{2}Cx_{HA}^2 + (2B + 3C)x_{HA} - (B + C + \ln K) \tag{12}$$

Since $\ln s'$ is known for various values of x_{HA}, the experimental data can be fitted to Equation (12) by quadratic least-squares. The coefficients thus determined can then be used to find B, C, the values of γ_{HA} and γ_{HB}, and K.

Returning to the general situation where neither B_l nor B_s is zero, but where Equations (7) and (8) are valid, we note the interesting and crucial fact that a plot of $\ln(x_A/x_B)$ as ordinate against $x_A - x_B$ as abscissa, although sigmoidal in shape, has a nearly linear portion between approximately $x_A - x_B = -0.50$ and $+0.50$, that is, between $x_A = 0.25$ and 0.75, or R between 0.3 and 3. The line also passes through the origin. Within this range, therefore, $\ln(x_A/x_B)$ is nearly proportional to $(x_A - x_B)$, or $\ln(x_A/x_B) \cong k(x_A - x_B)$, with k in the neighborhood of 2.14. Acceptance of this simplification means that, in Equation (4), $\ln(\gamma_{HB}/\gamma_{HA})$ can be replaced by $(B_s/2.14)\ln(x_{HA}/x_{HB})$ and $\ln(\gamma_B/\gamma_A)$ by $(B_s/2.14)\ln(x_{A(l)}/x_{B(l)})$, provided the data for *both* phases lie in the appropriate range. We have, then, $\ln K \cong \ln R_l - \ln R_s + (B_s/2.14)\ln R_s - (B_l/2.14)\ln R_l$, or

$$\ln R_s \cong \frac{2.14 - B_l}{2.14 - B_s}\ln R_l + \frac{2.14}{B_s - 2.14}\ln K \tag{13}$$

Comparison of this with Equation (1) shows that, if the experimental data lie in the

proper range, the slope m, which is always positive, may be identified with $(2.14 - B_l)/(2.14 - B_s)$ and the intercept with $[2.14/(B_s - 2.14)] \ln K$. Thus the slope is influenced by deviations in both the liquid and solid phases but the intercept by those in the solid phase only, and by the equilibrium constant. It is seen, therefore, that Equation (1) *does* have a theoretical justification. Clearly, if both B_l and B_s are zero, Equation (13) reduces to Equation (3), and if they are equal but non-zero the slope is still unity, the non-ideality of one phase cancelling that of the other. Furthermore, since $|B_l|$ and $|B_s|$ could never be larger than 2.14, then, if $B_l > B_s$ (algebraically), $m < 1$, and conversely. It is now evident why the oft used Equation (1) has seemed to be such a good representation of the experimental results in spite of probably considerable deviations from ideality. The experimental data are least accurate at low and high values of R, so that what may have been an actual curvature of the lines was attributed to experimental error and thus discounted, and the plot taken as linear. It must be admitted, that the distributions in many of the systems studied are so skewed that, although both $x_{A(l)}$ and x_{HA} cover a fairly wide range there are few data points where both lie in the required range for Equation (13) to be valid. Nevertheless, it is a surprisingly good approximation, as will be seen below.

We now return to the shape of that portion of the $\ln R_l/\ln R_s$ graph which joins the two limiting straight lines. This, of course, is the region where the experimental data lie. Any one system is characterized by the magnitudes of the three variables, B_l, B_s, and K. Twenty-seven (3^3) sets of calculations of $\ln R_l$ for arbitrary, closely spaced R_s values were performed using all possible combinations of $B_l = 0, 1$ and -1, $B_s = 0, 1$, and -1, and $K = 1, 1/3$, and 3 in Equation (2). It was thus determined that the shapes of the plots fall in one of the five categories which are denoted Types A, B, C, D, and E, and illustrated schematically in Figure 2. Table I gives the conditions producing each type. Types D and E occur when B_l and B_s are coincidentally equal or nearly equal. Except where $B_l = B_s \neq 0$, a change in K,

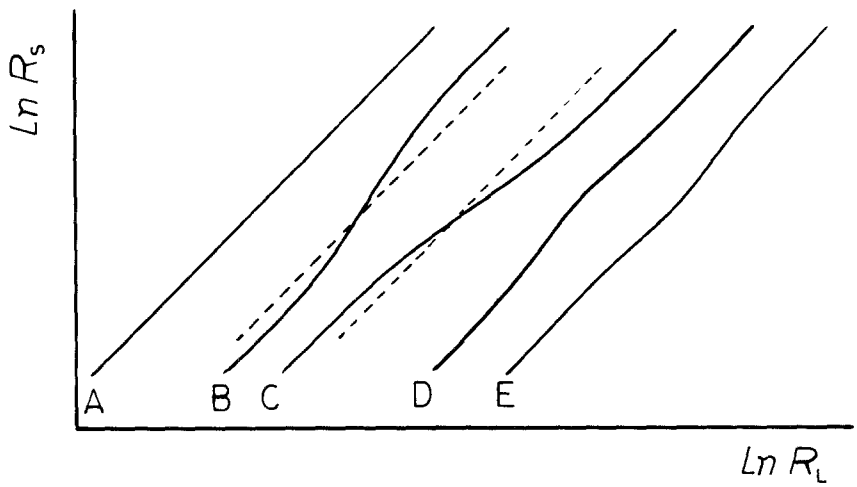

Fig. 2. Five types of graphs possible in distribution systems. The dashed lines indicate how a selectivity reversal could occur at the points of intersection.

Table I. The five types of graphical behaviour for $\ln R_l / \ln R_s$ plots.

Type	Shape	Conditions
A	linear	$B_l = B_s \neq 0, K = 1$; $B_l = B_s = 0$
B	sigmoidal	$B_l < B_s$
C	reverse sigmoidal	$B_l > B_s$
D	"positive ripple"	$B_l = B_s > 0, K < 1$; $B_l = B_s < 0, K > 1$
E	"negative ripple"	$B_l = B_s > 0, K > 1$; $B_l = B_s < 0, K < 1$

keeping B_l and B_s unchanged, causes the graph to be translated horizontally and/or vertically, thereby changing the intercepts on both axes. It should be emphasized that (1) any curvatures in Figure 2 are mild ones experimentally, (2) the linear end portions, all with unit slope, are well beyond the range of the experimental data, (3) the inequalities in Table I are algebraic ones, and (4) no attempt is made in the figure to imply the values of the intercepts on the axes. As the range of the experimental data lies in the curving portions in Types B to E, the measured slopes, m, are >1 for Type B, <1 for Type C, and not readily predictable for Types D and E.

A corollary to the preceding discussion concerns the three types of distribution described by Bakhius Roozeboom for complete series of solid solutions [8]. Distributions in which $R_l > R_s$ or $R_l < R_s$ throughout the entire range of composition were designated by him as Type I. Such behaviour would result if all the tie lines of Figure 1, when produced upwards, pass to the same side of the H apex or through it. In his Type II there is a region where the composition of the solid phase varies so much more rapidly than that of the coexisting liquid phase that the tie lines on the A side of the diagram, when produced upwards, pass to the left of the apex while those on the B side pass to the right side. Such behaviour suggests a *tendency* toward a break in the series of solid solutions (partial miscibility). In his Type III there is a region where the composition of the solid phase varies much more slowly than that of the coexisting liquid, so that the tie lines on the A side, when produced upwards, pass to the right of the apex while those on the B side pass to the left – suggesting a *tendency* toward the formation of a compound of HA and HB.

In comparing the Roozeboom classification with the types shown in Figure 2 it is to be noted that, if a system shows a selectivity reversal, as in the Roozeboom Types II and III, that is, if it has a tie line in Figure 1 where $R_l < R_s$ on one side but $R_l > R_s$ on the other, then the corresponding line of Figure 2 must intersect the 45° diagonal where $\ln R_l = \ln R_s$ and therefore $R_l = R_s$. There seems to be no *requirement* that this occur in any of the types, but it could occur in Types B and C. Thus Roozeboom's Type I could arise from Types A, B, or C; his Type II could arise in Type B, and Type III in Type C if the 45° diagonal of Figure 2 were to intersect the curved middle portion, as shown by the dashed lines. These conclusions are consistent with the requirements stated in Table I: for Type B, where $B_l < B_s$, large positive deviations from ideality in the solid phase would promote partial miscibility; for Type C, where the reverse is true, large negative deviations would be in line with possible compound formation between HA and HB.

3. Application to Solid Solutions of Inclusion Compounds of Ni(4-mepy)$_4$(NCS)$_2$

The foregoing treatment was applied to data for twelve systems (guest pairs) involving the host Ni(4-mepy)$_4$(NCS)$_2$, the most commonly studied host to date. The published data are in the form of pairs of R_l and R_s values for each system. As indicated later, some data points were rejected when, in the determination of B_s through Equation (11), it became apparent that they were subject to considerable error. Most of these points were for large values of R_l and/or R_s. In the pairs with *p*-dichlorobenzene and *p*-dibromobenzene the solid forms of these substances are encountered. To avoid their presence, only those regions of the system were studied where their concentrations are low.

The general procedure adopted for every system was to calculate s', plot $x_{HA} - x_{HB}$ against $\ln s'$, and determine the best straight line through the resulting points according to Equation (11). B_s and K for each guest pair determined in this way are shown in Table II. This permits the calculation of γ_{HA} and γ_{HB} through Equation (8). The standard free energy change at room temperature, ΔG^0_{rt}, calculated from K for the displacement of A from HA by B, is also listed.

The values of γ_A and γ_B needed in the above calculation were estimated by means of the Regular Solution Theory of Hildebrand [9], according to which

$$RT \ln \gamma_A = V^m_A \phi^2_B (\delta_A - \delta_B)^2; \qquad RT \ln \gamma_B = V^m_B \phi^2_A (\delta_A - \delta_B)^2$$

where V^m_A, V^m_B are the molar volumes of the respective guests, ϕ_A, ϕ_B their respective volume fractions, δ_A, δ_B their solubility parameters, and where R and T have their usual meaning. The solubility parameters used and their sources are included in Table II. It is recognized that Regular Solution Theory is less reliable for solutions containing polar components, but the results are presented for what they are worth. In any case, the polarity of the polar components is small except for *p*-fluoro-, *p*-chloro-, and *p*-bromotoluenes. Although γ_A and γ_B, determined in this way meet the requirements of the Gibbs–Duhem equation they are not necessarily expressible by Equations (7). Nevertheless, they can be approximately so expressed using the values of B_l given in Table II, which are included to convey some idea of the magnitude of the deviations from ideality in the liquid phase.

In the second and third systems listed, and in which A and B differ only isotopically, a cosolvent, pentane, had been used as a diluent. Although *p*-xylene-pentane solutions are not ideal – the solubility parameters for these components are 18.0 and 14.5 $J^{1/2}$ cm$^{-3/2}$, respectively – it is probably safe to assume that γ_A/γ_B is close to unity because of the similarity of isotopomers. For these two systems, then, B_l is assigned a value of zero.

It should be emphasized that the $\ln s'/(x_{A(s)} - x_{B(s)})$ graph is a severe test of the quality of the data. The considerable scatter in the points so obtained and/or a paucity of data indicate that the use of Equation (12) and the resulting quadratic fitting is a meaningless refinement for the present data.

The values of s needed in the above treatment were obtained without smoothing the original data, the smoothing process having been deferred until Equation (11) was applied. The possibility of smoothing the data initially, according to Equation (1), was considered, followed by application of Equation (11) to the smoothed data. It was felt preferable, however, since Equation (11) has a theoretical basis whereas

Table II. Calculated equilibrium constants and related data for the displacement of one guest (A) by another (B) in the host $Ni(4\text{-mepy})_4(NCS)_2$ at room temperature.

Guest pair A/B	Source of data Ref. no.	Fraction of data points used	δ_B $J^{1/2}\,cm^{-3/2}$	B_l	B_s	Type	K	ΔG^0_{rt} kJ/mol	b_{calc} Eq. (13)	b_{expt}	m_{calc} Eq. (13)	m_{expt}
p-xylene/ *p*-dibromobenzene	5	4/4	21.3[a,c]	0.5	1.12	B	3.6	−3.2	−2.7	−2.7	1.58	1.61
p-xylene/ *p*-xylene-d_6	3	16/16	18.0[c]	0	−0.04	C	1.13	−0.30	−0.12	−0.12	0.98	0.97
p-xylene/ *p*-xylene-d_{10}	3	18/18	18.0[c]	0	−0.05	C	1.10	−0.24	−0.09	−0.09	0.98	0.97
p-xylene/ *p*-bromotoluene	4	6/6	19.6[c]	0.14	+0.14	D	1.03	−0.073	−0.03	−0.03	1.00	1.00
(*p*-xylene/ *p*-xylene)	–	–	(18.0[b])				(1.00)					
p-xylene/ *p*-chlorotoluene	4	11/11	19.2[c]	0.07	0.07	D	0.99	+0.025	+0.001	+0.007	1.00	1.00
p-dichlorobenzene/ *p*-chlorotoluene	4	8/9	19.2[c]	0.05	0.05	D	0.98	+0.050	+0.02	+0.02	1.00	1.00
p-xylene/ *p*-dichlorobenzene	4	10/10	20.3[a,c]	0.24	0.14	C	0.87	+0.35	+0.15	+0.15	0.95	0.95
ethylbenzene/ toluene	2	8/9	18.2[b]	0.003	−1.6	C	0.22	+3.8	+0.87	+0.91	0.57	0.60
p-xylene/ *p*-fluorotoluene	4	9/10	18.2[c]	0	−1.4	C	0.20	+4.0	+0.97	+0.99	0.60	0.64
p-xylene/ ethylbenzene	2	7/11	18.0[b]	0	+0.62	B	0.15	+4.7	+2.67	+2.44	1.41	1.28
p-xylene/ toluene	2	6/9	18.2[b]	0	−1.4	C	0.069	+6.6	+1.62	+1.65	0.60	0.61
p-xylene/ benzene	4	4/5	18.8[b]	0.02	−10.0	C	1.2×10^{-5}	+28	+2.00	+2.58	0.17	0.34

[a] Values for metastable liquid.
[b] Ref. 9, p. 214.
[c] Calculated by author from energy of vaporization, density, and molecular weight.

Equation (1) is only an approximation, to use Equation (11) for the smoothing, and not to rely on Equation (1) for this purpose. Actually, there was little difference between the results from the two procedures.

In spite of the approximate nature of Equation (13) it was used to calculate m and b for each system. Table II includes the results and compares them with those found originally from Equation (1). The agreement is surprisingly good, considering the restrictions on the validity of Equation (13).

Inspection of Table II shows that, if one can accept the predictions of Regular Solution Theory, deviations from ideality in the liquid phase are zero or small for all but the systems containing p-xylene with p-dichlorobenzene, p-dibromobenzene, and p-bromotoluene. Deviations in the solid phase are all non-zero, being slightly negative for half of the systems reported and positive for the remainder. There seems to be no correlation between the magnitude of the deviations and the difference in the van der Waals lengths of the members of each guest pair. In over half of the systems $B_l > B_s$ (algebraically). The significance of this is not evident, but it gives lines with a slope <1 in $\ln R_l / \ln R_s$ plots, as shown above.

When, for a triad of guests (A, B, and C) K has been determined for all three guest pairs (A/B, A/C, B/C), a check on the consistency of the data is possible because K for the A/B pair ($K_{A/B}$) should equal $K_{A/C}/K_{B/C}$. Two such triads are A = p-xylene, B = p-dichlorobenzene, C = p-chlorotoluene and A = p-xylene, B = ethylbenzene, C = toluene. In the first triad, taking equilibrium constants from Table II, 0.87 is to be compared with 0.99/0.98 or 1.01; in the second 0.15 is to be compared with 0.069/0.22 or 0.31. The agreement leaves much to be desired. This test is a severe one, however, and is probably all that can be expected considering the scatter of much of the data when Equation (11) is applied to find B_s.

In conclusion, it is interesting to plot $\ln R_l$ against $\ln R_s$ using values calculated from B_l, B_s, and K given in Table II, in order to determine how well the raw data

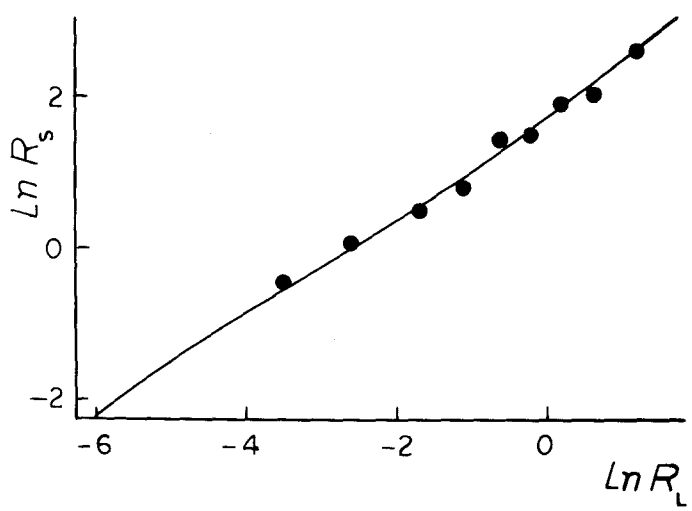

Fig. 3. Distribution plot in the system p-xylene–toluene–Ni(4-mepy)$_4$(NCS)$_2$ at room temperature. Line, calculated; points, experiment.

are reproduced and how sigmoidal is the resulting plot. For this purpose the system *p*-xylene/toluene was chosen because (1) the numerical value of $B_l - B_s$ is large (and therefore more likely to show the desired effect) and (2) at least six data points are available. With $B_l = 0.003$, $B_s = -1.4$, and $K = 0.069$, R_s was first found for rounded values of $x_{A(s)}$. Then s' was determined for each value of $x_{A(s)}$ using Equation (11), and s' corrected to s. Knowing R_s, R_l could be found. $\ln R_l$ was then plotted against $\ln R_s$ to give the slightly reverse sigmoidal curve shown in Figure 3 (Type C). The original raw data [3] are also shown as points on or near the line. Calculation shows that the latter points fit the mildly curved line better than the straight line to which they were originally fitted (Equation (1)). At the same time, however, the points are not far from a straight line and, for lack of further information, any deviations from a straight line could easily be mistaken for experimental error.

References

1. W. D. Schaeffer, W. S. Dorsey, D. A. Skinner, and C. G. Christian: *J. Am. Chem. Soc.* **79**, 5870 (1957).
2. Sr. M. J. Minton and N. O. Smith: *J. Phys. Chem.* **71**, 3618 (1967).
3. S. E. Ofodile and N. O. Smith: *J. Phys. Chem.* **87**, 473 (1983).
4. H. L. Wiener, L. Ilardi, P. Liberati, L. Dengler, S. A. Jeffas, S. Saba, and N. O. Smith: *J. Incl. Phenom.* **4**, 415 (1986).
5. J. Lipkowski, A. Zielenkiewicz, J. Hatt, and W. Zielenkiewicz: *J. Incl. Phenom.* **7**, 511 (1989).
6. J. M. Prausnitz: *Molecular Thermodynamics of Fluid-Phase Equilibria*, p. 209. Prentice-Hall, Inc., Englewood Cliffs, N.J. (1969).
7. Ref. [6], p. 202.
8. H. W. Bakhius Roozeboom: *Z. Phys. Chem.* **8**, 521 (1891).
9. J. H. Hildebrand, J. M. Prausnitz, and R. L. Scott: *Regular and Related Solutions*, p. 87. Van Nostrand Reinhold Co., N.Y. (1970).